

Transport Properties of Dirac Ferromagnet

Junji Fujimoto^{1,*} and Hiroshi Kohno^{2,†}

¹*Department of Materials Engineering Science, Osaka University,
Machikaneyama 1-3, Toyonaka, Osaka 560-8531 Japan*

²*Department of Physics, Nagoya University, Furo-cho, Chikusa-ku, Nagoya, 464-8601, Japan*
(Dated: December 3, 2024)

We propose a model ferromagnet based on the Dirac Hamiltonian in three spatial dimensions, and study its transport properties which include anisotropic magnetoresistance (AMR) and anomalous Hall (AH) effect. This relativistic extension allows two kinds of ferromagnetic order parameters, denoted by \mathbf{M} and \mathbf{S} , which are distinguished by the relative sign between the positive- and negative-energy states (at zero momentum) and become degenerate in the non-relativistic limit. Because of the relativistic coupling between the spin and the orbital motion, both \mathbf{M} and \mathbf{S} induce anisotropic deformations of the energy dispersion (and the Fermi surfaces) but in mutually opposite ways. The AMR is determined primarily by the anisotropy of the Fermi surface (group velocity), and secondarily by the anisotropy of the damping; the latter becomes important for $\mathbf{M} = \pm\mathbf{S}$, where the Fermi surfaces are isotropic. Even when the chemical potential lies in the gap, the AH conductivity is found to take a finite non-quantized value, $\sigma_{ij} = -(\alpha/3\pi^2\hbar)\epsilon_{ijk}S_k$, where α is the (effective) fine structure constant. This offers an example of Hall insulator in three spatial dimensions.

PACS numbers: 72.25.-b, 71.15.Rf

I. INTRODUCTION

Recently, spintronics is an active area of research with fundamental as well as applicational interest. In spintronic phenomena based on ferromagnetic materials, one of the central interests is the interaction between electric current and magnetization, such as giant magnetoresistance and electrical manipulation of magnetization. While these phenomena do not require spin-orbit coupling (SOC) in principle, they are expected to acquire new features in the presence of SOC. It is thus important to study the effects of SOC on various phenomena in spintronics.

As one of the simplest models of ferromagnetism containing SOC, we propose in this paper a Stoner-like model based on the Dirac Hamiltonian in three spatial dimensions (3D). Such models of ferromagnetism (with relativistic effects) have been considered previously in two different ways. One, introduced by MacDonald and Vosko,¹ is characterized by a ferromagnetic order parameter (which we represent by \mathbf{M} in this paper) having opposite signs between the positive- and negative-energy states. The other, proposed by Ramana and Rajagopal,² is described by an order parameter (denoted by \mathbf{S} in this paper) having the same sign in both states. In *ab initio* calculations, the former has been used mainly.^{3,4} In view of the fact that the ferromagnetism arises as a spontaneous symmetry breaking, however, there seems to be no reason to exclude either of the two order parameters *a priori*. Based on this observation, we propose a model which contains both \mathbf{M} and \mathbf{S} in general. In the following, we call this model a “Dirac ferromagnet” for brevity.

While the present model was originally motivated by the true relativistic effect (“true” Dirac model), it would find more appropriate applications to electrons in solids as an effective model (“effective” Dirac model). It is

known that electrons in some materials, such as bismuth⁵ and bulk states of 3D topological insulators,⁶ are described by an effective Dirac-type Hamiltonian. If such materials become ferromagnetic, for example by doping magnetic impurities, they will be described as a Dirac ferromagnet. Candidate materials would be Mn-doped $\text{Bi}_2(\text{Se},\text{Te})_3$ ^{7,8} and Cr-doped $(\text{Bi},\text{Sb})_2\text{Te}_3$.^{9,10}

In this paper, we study magneto-transport properties of the Dirac ferromagnet in its homogeneous state, which include anisotropic magnetoresistance (AMR)^{11–14} and anomalous Hall effect (AHE)^{15–17}. While we present a general formulation by retaining both \mathbf{M} and \mathbf{S} , explicit results will be demonstrated mostly for three typical cases; (i) $\mathbf{S} = \mathbf{0}$, (ii) $\mathbf{M} = \mathbf{0}$, and (iii) $\mathbf{M} = \mathbf{S}$. Two factors have been identified that determine the AMR, the anisotropy of the Fermi surface (group velocity) and the anisotropy of the damping. In general, the former effect is much stronger than the latter, but in case $\mathbf{M} = \mathbf{S}$, where the Fermi surfaces are isotropic, AMR is determined by the latter. As for AHE, we found a new type of Hall insulator state in which the Hall conductivity is finite and proportional to \mathbf{S} (hence not quantized) while the longitudinal conductivity vanishes. This may explain the peculiar behavior of Cr-doped $(\text{Bi},\text{Sb})_2\text{Te}_3$ found recently.¹⁰

This paper is organized as follows. We define the model in Sec. II and calculate the conductivity tensor in Sec. III. The main results are presented in Sec. IV, where AMR and the anomalous Hall (AH) conductivity are shown for the three typical cases, (i)–(iii), and the key factors are discussed. Summary is given in Sec. V. Some details of the calculation are presented in the Appendices. Appendix A gives the damping constants explicitly, and Appendices B to D give the calculation of AH conductivity for the three cases, respectively. Symmetry properties of the conductivity tensor are studied in Appendix E.

II. MODEL AND GREEN'S FUNCTION

A. Model

We consider an electron system described by a 4×4 Dirac Hamiltonian with additional two kinds of ferromagnetic order parameters, \mathbf{M} and \mathbf{S} ,

$$\mathcal{H}_0 = \hbar c \mathbf{k} \cdot \boldsymbol{\sigma} \rho_1 + mc^2 \rho_3 - \mathbf{M} \cdot \boldsymbol{\sigma} \rho_3 - \mathbf{S} \cdot \boldsymbol{\sigma}, \quad (1)$$

and subject to impurity potentials,

$$V_{\text{imp}}(\mathbf{r}) = u \sum_i \delta(\mathbf{r} - \mathbf{R}_i). \quad (2)$$

Here $\boldsymbol{\sigma} = (\sigma^x, \sigma^y, \sigma^z)$ are the Pauli matrices in spin space, ρ_i ($i = 1, 2, 3$) are the Pauli matrices in electron-positron (particle-hole) space, and m , c and \mathbf{k} are the mass, velocity and wave vector, respectively, of a Dirac particle. The total Hamiltonian is given by

$$H_{\text{tot}} = \sum_{\mathbf{k}} \psi_{\mathbf{k}}^\dagger (\mathcal{H}_0 - \mu) \psi_{\mathbf{k}} + \int d\mathbf{r} \psi^\dagger(\mathbf{r}) V_{\text{imp}}(\mathbf{r}) \psi(\mathbf{r}), \quad (3)$$

where $\psi(\mathbf{r})$ is a four-component Dirac spinor field, $\psi_{\mathbf{k}}$ is its Fourier transform, and μ is the chemical potential. We treat the impurity potential V_{imp} perturbatively in the Born approximation (see the next subsection). In the following calculations, we put $c = \hbar = 1$ and recover them in the results.

Because of the ρ_3 matrix, \mathbf{M} acts oppositely between the positive- and negative-energy states (at $\mathbf{k} = \mathbf{0}$),¹⁸ whereas \mathbf{S} acts with the same sign. In the “true” Dirac model, \mathbf{M} physically represents “magnetization” and couples to real magnetic fields whereas \mathbf{S} represents “spin”, which would not couple to any physical fields.¹⁹ Note, however, that this does not mean that \mathbf{S} is unphysical and unsuitable for an order parameter as suggested in Ref. 3. This is because a ferromagnetism arises as a spontaneous symmetry breaking, which is governed by the content of the interaction.²⁰

When the ferromagnetism is driven by magnetic doping in solids (“effective” Dirac model), the resulting order parameter will be \mathbf{S} (\mathbf{M}) if the exchange interaction of Dirac particles with the magnetic impurity have the same (opposite) sign between the positive-energy state (conduction band) and negative-energy state (valence band).²¹

In this paper, we assume that the order parameters are given. We restrict ourselves to the case that \mathbf{M} and \mathbf{S} are uniform and mutually parallel, and take the z -axis along their direction, $\mathbf{M} = M\hat{z}$, $\mathbf{S} = S\hat{z}$. In addition, we assume that $M + S < m$ to avoid the closing of the original gap (due to m); see below. The values of M and S are otherwise arbitrary, but some explicit results will be displayed for the following three typical cases;

$$(i) \quad \mathbf{M} = M\hat{z}, \mathbf{S} = \mathbf{0},$$

$$(ii) \quad \mathbf{M} = \mathbf{0}, \mathbf{S} = S\hat{z},$$

$$(iii) \quad \mathbf{M} = \mathbf{S} = S\hat{z}.$$

In these special cases, the energy dispersion takes relatively simple forms,

$$\zeta \sqrt{k^2 + m^2 + M^2 + 2\eta M \sqrt{k_\perp^2 + m^2}}, \quad (4)$$

$$\zeta \sqrt{k^2 + m^2 + S^2 + 2\eta S \sqrt{k_z^2 + m^2}}, \quad (5)$$

$$\zeta \sqrt{k^2 + (m + \eta S)^2} + \eta S, \quad (6)$$

for (i), (ii) and (iii), respectively, where $k_\perp^2 = k_x^2 + k_y^2$. (See Eqs. (B3), (C3) and (D3).) Here, $\zeta = \pm 1$ specifies positive/negative energy states, and $\eta = \pm 1$ specifies spin states. Figure 1(a) shows the energy dispersion for case (i). The Fermi surfaces at $\mu/m = 2.5$ are shown in Fig. 1(b) for the three cases. In contrast to ordinary (non-relativistic) ferromagnets, such as the Stoner model, Fermi surfaces are deformed in cases (i) and (ii) by the presence of ferromagnetic order parameters and become anisotropic. The anisotropy is opposite between the two Fermi surfaces in each case, and between the two cases (i) and (ii). Such anisotropic deformation of the Fermi surfaces due to ferromagnetism and SOC has been noted in ferromagnets with Dirac-,³ Luttinger-²² and Rashba-type²³ SOC. In case (iii), the Fermi surfaces remain isotropic.

B. Green's function

The unperturbed Green's function $G_{\mathbf{k}}^{(0)}(\epsilon) = (\epsilon - \mathcal{H}_0)^{-1}$ can be expressed as

$$G_{\mathbf{k}}^{(0)}(\epsilon) = \frac{1}{D_{\mathbf{k}}(\epsilon)} \sum_{\substack{\mu=0,1,2,3 \\ \nu=0,x,y,z}} g_{\mu\nu}^{(0)}(\epsilon) \rho_\mu \sigma_\nu, \quad (7)$$

where σ^0 and ρ_0 are unit matrices. We have defined

$$D_{\mathbf{k}}(\epsilon) = (\epsilon^2 - k^2 - m^2 - S^2 + M^2)^2 - 4\{(\epsilon M + mS)^2 + (S^2 - M^2)k_z^2\} \quad (8)$$

$$= \{\epsilon^2 - \epsilon_k^2 - 2\Delta_{\mathbf{k}}(\epsilon)\} \{\epsilon^2 - \epsilon_k^2 + 2\Delta_{\mathbf{k}}(\epsilon)\}, \quad (9)$$

$$\epsilon_k = \sqrt{k^2 + m^2 + S^2 - M^2}, \quad (10)$$

$$\Delta_{\mathbf{k}}(\epsilon) = \sqrt{\Omega^2 + (S^2 - M^2)k_z^2}, \quad (11)$$

$$\Omega = \epsilon M + mS, \quad (12)$$

and $g_{\mu\nu}^{(0)}(\epsilon)$'s are listed in Table I.

We evaluate the self-energy due to impurity scattering in the first Born approximation,

$$\Sigma^{\text{R}}(\epsilon) = n_i u^2 \sum_{\mathbf{k}} G_{\mathbf{k}}^{(0)}(\epsilon + i0), \quad (13)$$

where n_i is the concentration of impurities. Neglecting the real part, we consider only the imaginary part, which is calculated as

$$\text{Im } \Sigma^{\text{R}}(\epsilon) = - \sum_{\mu,\nu} \gamma_{\mu\nu}(\epsilon) \rho_\mu \sigma_\nu, \quad (14)$$

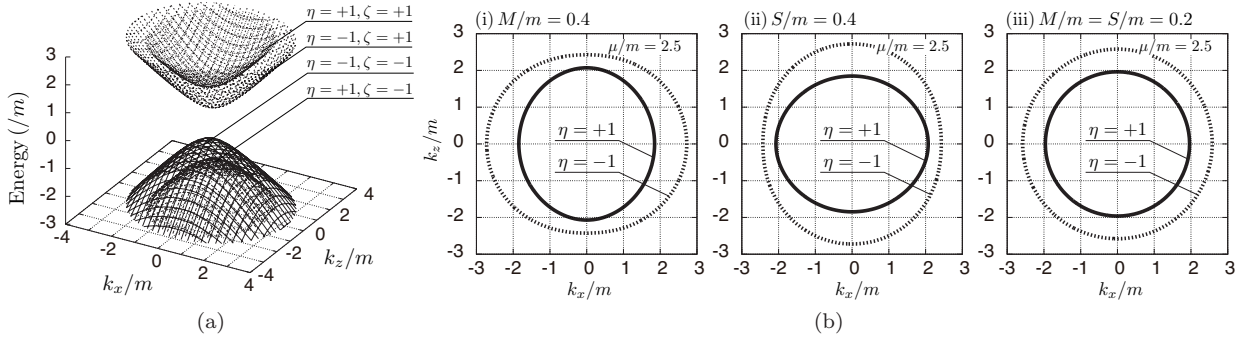


FIG. 1: Energy dispersion and Fermi surfaces for $\mathbf{M} = M\hat{z}$ and $\mathbf{S} = S\hat{z}$. (a) Energy dispersion for $M = 0.4m, S = 0$ (case (i)) plotted against k_z and k_x (or k_y). The $\eta = \pm 1$ specifies spin, and $\zeta = \pm 1$ specifies upper/lower Dirac bands (positive/negative energy states). (b) Fermi surfaces for the three typical cases, (i)–(iii).

TABLE I: The coefficients $g_{\mu\nu}^{(0)}$ of the unperturbed Green's function $G_{\mathbf{k}}^{(0)}(\epsilon)$ for $\mathbf{M} = M\hat{z}$ and $\mathbf{S} = S\hat{z}$.

(μ, ν)	0	x	y	z
0	$\epsilon(\epsilon^2 - \epsilon_k^2) - 2M\Omega$	$-2Sk_z k_x$	$-2Sk_z k_y$	$-S(\epsilon^2 - \epsilon_k^2 + 2k_z^2) - 2m\Omega$
1	$-2(\epsilon S + mM)k_z$	$(\epsilon^2 - \epsilon_k^2)k_x$	$(\epsilon^2 - \epsilon_k^2)k_y$	$k_z(\epsilon^2 - \epsilon_k^2 + 2S^2 - 2M^2)$
2	0	$-2\Omega k_y$	$2\Omega k_x$	0
3	$m(\epsilon^2 - \epsilon_k^2) + 2S\Omega$	$2Mk_z k_x$	$2Mk_z k_y$	$M(\epsilon^2 - \epsilon_k^2 + 2k_z^2) - 2\epsilon\Omega$

with

$$\gamma_{\mu\nu}(\epsilon) = -n_i u^2 \sum_{\mathbf{k}} \text{Im} \frac{1}{D_{\mathbf{k}}(\epsilon + i0)} g_{\mu\nu}^{(0)}(\epsilon). \quad (15)$$

Only the four components, $(\mu, \nu) = (0, 0), (0, z), (3, 0)$ and $(3, z)$, are finite and others vanish by symmetry. (See Appendix A for explicit results.) The renormalized (retarded) Green's function is expressed as

$$\begin{aligned} \{G_{\mathbf{k}}^{\text{R}}(\epsilon)\}^{-1} &= \epsilon - \mathcal{H}_0 - i \text{Im} \Sigma^{\text{R}}(\epsilon) \\ &= \epsilon + i\gamma_{00} - \rho_1 \mathbf{k} \cdot \boldsymbol{\sigma} - (m - i\gamma_{30})\rho_3 \\ &\quad + (M + i\gamma_{3z})\rho_3 \sigma^z + (S + i\gamma_{0z})\sigma^z. \end{aligned} \quad (16)$$

This is obtained from $G_{\mathbf{k}}^{(0)}(\epsilon)$ by the replacements, $\epsilon \rightarrow \epsilon + i\gamma_{00}, m \rightarrow m - i\gamma_{30}, S \rightarrow S + i\gamma_{0z}, M \rightarrow M + i\gamma_{3z}$. Let us write the denominator $D_{\mathbf{k}}^{\text{R}}(\epsilon)$ as

$$D_{\mathbf{k}}^{\text{R}}(\epsilon) = D' + iD'', \quad (17)$$

with the real (D') and imaginary (D'') parts, which are given by

$$D' = D_{\mathbf{k}} + \mathcal{O}(\gamma^2), \quad (18)$$

$$D'' = 4\{(\epsilon^2 - \epsilon_k^2)\Gamma_1 - 2\Omega\Gamma_2 - 2k_z^2\Gamma_3\} + \mathcal{O}(\gamma^3), \quad (19)$$

$$\Gamma_1 = \epsilon\gamma_{00} + m\gamma_{30} - S\gamma_{0z} + M\gamma_{3z}, \quad (20)$$

$$\Gamma_2 = M\gamma_{00} - S\gamma_{30} + m\gamma_{0z} + \epsilon\gamma_{3z}, \quad (21)$$

$$\Gamma_3 = S\gamma_{0z} - M\gamma_{3z}. \quad (22)$$

In this paper, we assume that the effects of impurity scattering are weak, and calculate the conductivity tensor in

the leading order with respect to the damping parameters $\gamma_{\mu\nu}$, which are collectively denoted as γ in the following as well as in Eqs. (18) and (19), where terms of $\mathcal{O}(\gamma^2)$ and $\mathcal{O}(\gamma^3)$, respectively, or higher are suppressed.

III. CALCULATION OF CONDUCTIVITY

The dc conductivity tensor σ_{ij} ($i, j = x, y, z$) is given by the Kubo formula²⁴ as

$$\sigma_{ij} = \lim_{\omega \rightarrow 0} \frac{Q_{ij}^{\text{R}}(\omega) - Q_{ij}^{\text{R}}(0)}{i\omega}, \quad (23)$$

where $Q_{ij}^{\text{R}}(\omega)$ is the current-current retarded response function. In this paper, we neglect vertex corrections and evaluate it from

$$Q_{ij}(i\omega_\lambda) = -e^2 T \sum_n \sum_{\mathbf{k}} \text{tr} \left[v_i \tilde{G}_{\mathbf{k}}(i\epsilon_n + i\omega_\lambda) v_j \tilde{G}_{\mathbf{k}}(i\epsilon_n) \right], \quad (24)$$

via the analytic continuation, $i\omega_\lambda \rightarrow \omega + i0$, where $\epsilon_n = (2n + 1)\pi T$ and $\omega_\lambda = 2\lambda\pi T$ are Matsubara frequencies, and

$$\mathbf{v} = \rho_1 \boldsymbol{\sigma} \quad (25)$$

is the velocity matrix. In Eq. (24), we have defined

$$\tilde{G}_{\mathbf{k}}(i\epsilon_n) = (i\epsilon_n + \mu - \mathcal{H}_0 - \Sigma(i\epsilon_n))^{-1}, \quad (26)$$

where $\Sigma(i\epsilon_n)$ and $\Sigma^{\text{R}}(\epsilon)$ [Eq. (13)] are mutually related via the analytic continuation. (This $\tilde{G}_{\mathbf{k}}(i\epsilon_n)$ differs from

$G_{\mathbf{k}}(i\epsilon_n)$ only in the presence of μ .) The temperature T is assumed to be zero, $T = 0$, throughout. The result is written as

$$\sigma_{ij} = \sigma_{ij}^{(1)} + \sigma_{ij}^{(2)} + \sigma_{ij}^{(3)}, \quad (27)$$

with

$$\sigma_{ij}^{(1)} = -\frac{e^2}{4\pi} \sum_{\mathbf{k}} \text{tr} [v_i (G_{\mathbf{k}}^{\text{R}}(\epsilon) - G_{\mathbf{k}}^{\text{A}}(\epsilon)) v_j (G_{\mathbf{k}}^{\text{R}}(\epsilon) - G_{\mathbf{k}}^{\text{A}}(\epsilon))] \Big|_{\epsilon=\mu}, \quad (28)$$

$$\sigma_{ij}^{(2)} = \frac{e^2}{4\pi} \sum_{\mathbf{k}} \text{tr} [v_i G_{\mathbf{k}}^{\text{R}}(\epsilon) v_j G_{\mathbf{k}}^{\text{A}}(\epsilon) - v_i G_{\mathbf{k}}^{\text{A}}(\epsilon) v_j G_{\mathbf{k}}^{\text{R}}(\epsilon)] \Big|_{\epsilon=\mu}, \quad (29)$$

$$\sigma_{ij}^{(3)} = -\frac{e^2}{4\pi} \sum_{\mathbf{k}} \int_{-\infty}^{\mu} d\epsilon \lim_{\epsilon' \rightarrow \epsilon} (\partial_{\epsilon} - \partial_{\epsilon'}) \text{tr} [v_i G_{\mathbf{k}}^{\text{R}}(\epsilon) v_j G_{\mathbf{k}}^{\text{R}}(\epsilon') - v_i G_{\mathbf{k}}^{\text{A}}(\epsilon) v_j G_{\mathbf{k}}^{\text{A}}(\epsilon')]. \quad (30)$$

Here, $\sigma_{ij}^{(1)}$ is symmetric with respect to i and j and contributes to the longitudinal conductivity, whereas $\sigma_{ij}^{(2)}$ and $\sigma_{ij}^{(3)}$ are anti-symmetric and contribute to the Hall conductivity. Because of the remaining ϵ -integral, $\sigma_{ij}^{(3)}$ is often called a “Fermi-sea term”, whereas $\sigma_{ij}^{(1)}$ and $\sigma_{ij}^{(2)}$ are called “Fermi-surface terms”.²⁵ In the present model, only the diagonal components are finite for $\sigma_{ij}^{(1)}$ by symmetry.

As stated above, we calculate σ_{ij} in the leading order with respect to the damping parameters $\gamma_{\mu\nu}$, which are $\mathcal{O}(\gamma^{-1})$ for the longitudinal conductivity, and $\mathcal{O}(\gamma^0)$ for the Hall conductivity.

A. AMR

We first consider the symmetric part, $\sigma_{ij}^{(1)}$. Putting $\sigma_{\perp} \equiv \sigma_{xx}$ ($= \sigma_{yy}$) and $\sigma_{\parallel} \equiv \sigma_{zz}$, the difference $\Delta\sigma = \sigma_{\perp} - \sigma_{\parallel}$ defines AMR. Substituting the Green’s function (16) in the form of Eq. (7) into Eq. (28), dropping the damping in the numerator as $g_{\mu\nu}^{\text{R(A)}}(\epsilon) \simeq g_{\mu\nu}^{(0)}(\epsilon)$, taking the traces of ρ_{μ} and σ^{ν} matrices, and using

$$\left(\frac{1}{D_{\mathbf{k}}^{\text{R}}} - \frac{1}{D_{\mathbf{k}}^{\text{A}}} \right)^2 = -4 \left[\frac{D''}{(D')^2 + (D'')^2} \right]^2 \simeq -\frac{2\pi}{|D''|} \delta(D'), \quad (31)$$

$\sigma_{ij}^{(1)}$ is expressed as

$$\sigma_{ij}^{(1)} = 2e^2 \sum_{\mathbf{k}} \left(C^{(1)} \delta_{ij} + C_{ij}^{(2)} \right) \frac{\delta(D')}{|D''|} \Big|_{\epsilon=\mu}, \quad (32)$$

where δ_{ij} is the Kronecker’s delta, and

$$C^{(1)} = \sum_{\mu,\nu} s_{\mu} \eta_{\nu} g_{\mu\nu}^{(0)}(\epsilon) g_{\mu\nu}^{(0)}(\epsilon), \quad (33)$$

$$C_{ij}^{(2)} = \sum_{\mu} 2s_{\mu} g_{\mu i}^{(0)}(\epsilon) g_{\mu j}^{(0)}(\epsilon), \quad (34)$$

with

$$s_{\mu} = \begin{cases} 1 & (\mu = 0, 1) \\ -1 & (\mu = 2, 3), \end{cases} \quad (35)$$

$$\eta_{\nu} = \begin{cases} 1 & (\nu = 0) \\ -1 & (\nu = x, y, z). \end{cases} \quad (36)$$

Explicitly, $C^{(1)}$ and $C_{ij}^{(2)}$ ’s are given by

$$C^{(1)} = (\epsilon^2 - \epsilon_{\mathbf{k}}^2) D_{\mathbf{k}} + 8k_{\perp}^2 \Omega^2, \quad (37)$$

$$C_{\perp}^{(2)} = k_{\perp}^2 \{ D_{\mathbf{k}} + 8k_z^2 (S^2 - M^2) \}, \quad (38)$$

$$C_{\parallel}^{(2)} = 2(S^2 - M^2 + k_z^2) D_{\mathbf{k}} + 8\Omega^2 (2k_z^2 - k_{\perp}^2) + 16k_z^2 (S^2 - M^2) (\epsilon^2 - k_{\perp}^2 - m^2), \quad (39)$$

where $C_{\perp}^{(2)} \equiv (C_{xx}^{(2)} + C_{yy}^{(2)})/2$ and $C_{\parallel}^{(2)} \equiv C_{zz}^{(2)}$. The δ -function is resolved as

$$\delta(D') \simeq \delta(D_{\mathbf{k}}) = \sum_{\eta=\pm} \frac{\delta(k_{\perp}^2 - \alpha_{\eta})}{4\Delta_{\mathbf{k}}(\epsilon)} \Theta_{\eta}(\epsilon), \quad (40)$$

where

$$\alpha_{\eta} = \epsilon^2 - k_z^2 - m^2 - S^2 + M^2 - 2\eta\Delta_{\mathbf{k}}(\epsilon), \quad (41)$$

and the function

$$\Theta_{\eta}(\epsilon) = \begin{cases} 1 & (\epsilon < -m - \eta|S - M| \text{ or } \epsilon > m + \eta(S + M)) \\ 0 & (\text{otherwise}) \end{cases} \quad (42)$$

assures $\alpha_\eta > 0$. Using $\mu^2 - \epsilon_k^2 = 2\eta\Delta_{\mathbf{k}}$ ensured by the δ -function in Eq. (40), with

$$\Delta_{\mathbf{k}} \equiv \Delta_{\mathbf{k}}(\epsilon = \mu), \quad (43)$$

we obtain

$$\sigma_A = \frac{e^2}{2(2\pi)^2} \sum_{\eta} \Theta_{\eta}(\mu) \int_0^{\xi_{\eta}} dk_z \frac{C_A}{|\eta\Delta_{\mathbf{k}}\Gamma_1 - \Omega\Gamma_2 - k_z^2\Gamma_3|}, \quad (44)$$

for $A = \perp, \parallel$, where

$$C_{\perp} = \alpha_{\eta}\Delta_{\mathbf{k}}, \quad (45)$$

$$C_{\parallel} = 2k_z^2(\eta\Delta_{\mathbf{k}} + S^2 - M^2)^2/\Delta_{\mathbf{k}}, \quad (46)$$

and $\xi_{\eta} \equiv \xi_{\eta}(\epsilon = \mu)$ with

$$\xi_{\eta}(\epsilon) = \sqrt{\epsilon^2 - m^2 + S^2 - M^2 - 2\eta|mM + \epsilon S|}. \quad (47)$$

The remaining k_z -integral is performed numerically. The results, plotted in Figs. 2 and 3 for the three typical cases and in Fig. 4 for close neighbors of case (iii), will be discussed in Sec. IV.

B. AHE

We next look at the anti-symmetric parts, $\sigma_{ij}^{(2)}$ and $\sigma_{ij}^{(3)}$. For the Fermi-surface term, $\sigma_{ij}^{(2)}$, the leading-order contributions are $\mathcal{O}(\gamma^0)$, because both the numerator and the denominator are $\mathcal{O}(\gamma)$. Since there are four kinds of damping parameters [see Eq. (A3d)], we cannot evaluate $\sigma_{ij}^{(2)}$ by dropping them; their ratio determines the value of $\sigma_{ij}^{(2)}$. Substituting $G_{\mathbf{k}}^{R(A)}$ into Eq. (29) and taking the trace, we obtain

$$\sigma_{ij}^{(2)} = -\frac{4e^2}{\pi} \sum_{\mathbf{k}} \frac{1}{|D_{\mathbf{k}}^R(\epsilon)|^2} \sum_{\mu, k} \varepsilon_{ijk} s_{\mu} \text{Im} [g_{\mu 0}^R(\epsilon) g_{\mu k}^A(\epsilon)] \Big|_{\epsilon=\mu}, \quad (48)$$

where ε_{ijk} ($i, j, k = x, y, z$) is the Levi-Civita symbol in 3D, and $\sigma_{ij}^{(2)}$ can be nonzero only for $(i, j) = (x, y)$ or (y, x) . To the leading order in γ , we approximate as

$$\frac{1}{|D_{\mathbf{k}}^R(\epsilon)|^2} = \frac{1}{(D')^2 + (D'')^2} \simeq \frac{\pi}{|D''|} \delta(D'), \quad (49)$$

and

$$\sum_{\mu=0}^3 s_{\mu} \text{Im} [g_{\mu 0}^R(\epsilon) g_{\mu z}^A(\epsilon)] = -8\eta\Delta_{\mathbf{k}} C_{xy} + \mathcal{O}(\gamma^3), \quad (50)$$

with

$$\begin{aligned} C_{xy} = & \gamma_{00}(m\Omega + Sk_z^2 + \eta S\Delta_{\mathbf{k}}) \\ & + \gamma_{30}(\epsilon\Omega - Mk_z^2 - \eta M\Delta_{\mathbf{k}}) \\ & + \gamma_{0z}(M\Omega - \eta\epsilon\Delta_{\mathbf{k}}) \\ & - \gamma_{3z}(S\Omega + \eta m\Delta_{\mathbf{k}}). \end{aligned} \quad (51)$$

Here, we have put $D_{\mathbf{k}} = 0$ because of $\delta(D')$ [Eq. (49)], and used $\mu^2 - \epsilon_k^2 = 2\eta\Delta_{\mathbf{k}}$ from Eq. (40). Therefore, we obtain

$$\sigma_{xy}^{(2)} = \frac{e^2}{(2\pi)^2} \sum_{\eta} \eta \Theta_{\eta}(\mu) \int_0^{\xi_{\eta}} dk_z \frac{C_{xy}}{|\eta\Delta_{\mathbf{k}}\Gamma_1 - \Omega\Gamma_2 - k_z^2\Gamma_3|}, \quad (52)$$

where ξ_{η} is given by Eq. (47) with $\epsilon = \mu$. The remaining k_z -integral is performed numerically and the results are plotted in Fig. 5 for the three typical cases. This is an extrinsic contribution^{3,17} since it can only be obtained in the limit $\omega/\gamma \rightarrow 0$.^{17,26}

The Fermi-sea term $\sigma_{ij}^{(3)}$, which is also $\mathcal{O}(\gamma^0)$, can be evaluated by dropping all the damping constants. This is an intrinsic contribution^{3,17} since it survives in the ‘clean’ limit $\gamma/\omega \rightarrow 0$.¹⁷ Thus we consider

$$\sigma_{ij}^{(3)} = \frac{4e^2}{\pi} \sum_{\mathbf{k}} \int_{-\infty}^{\mu} d\epsilon \text{Im} \left[\frac{1}{D_{\mathbf{k}}^R(\epsilon)^2} \right] \sum_{\mu=0}^3 s_{\mu} \sum_{k=x,y,z} \varepsilon_{ijk} \left\{ \left(\partial_{\epsilon} g_{\mu 0}^{(0)}(\epsilon) \right) g_{\mu k}^{(0)}(\epsilon) - g_{\mu 0}^{(0)}(\epsilon) \left(\partial_{\epsilon} g_{\mu k}^{(0)}(\epsilon) \right) \right\}. \quad (53)$$

This vanishes unless $(i, j) = (x, y)$ or (y, x) as in the case

of $\sigma_{ij}^{(2)}$. We write

$$\begin{aligned} \text{Im} \left[\frac{1}{D_{\mathbf{k}}^R(\epsilon)^2} \right] &= \frac{\partial}{\partial D'} \frac{D''}{(D')^2 + (D'')^2} \\ &\simeq \pi \text{sign}(D'') \frac{\partial}{\partial D'} \delta(D'), \end{aligned} \quad (54)$$

and resolve the derivative of the δ -function as

$$\begin{aligned}\frac{\partial}{\partial D'}\delta(D') &= \frac{\partial\epsilon}{\partial D'}\frac{\partial}{\partial\epsilon}\delta(D') \\ &= \frac{1}{\partial_\epsilon D_{\mathbf{k}}}\frac{\partial}{\partial\epsilon}\left(\sum_i \frac{\delta(\epsilon - \epsilon_i)}{|\partial_\epsilon D_{\mathbf{k}}|_{\epsilon=\epsilon_i}}\right),\end{aligned}\quad (55)$$

where $\epsilon = \epsilon_i$ ($i = 1, \dots, 4$) are the roots of $D'(\epsilon) \simeq D_{\mathbf{k}}(\epsilon) = 0$. Putting

$$\begin{aligned}X(\epsilon) &\equiv \sum_{\mu=0}^3 s_\mu \left\{ (\partial_\epsilon g_{\mu 0}(\epsilon)) g_{\mu z}(\epsilon) - g_{\mu 0}(\epsilon) (\partial_\epsilon g_{\mu z}(\epsilon)) \right\} \\ &= -SD_{\mathbf{k}} - 8S[\Delta_{\mathbf{k}}(\epsilon)]^2 - 4(Sk_z^2 + m\Omega)(\epsilon^2 - \epsilon_k^2),\end{aligned}\quad (56)$$

and integrating by parts, we obtain²⁷

$$\begin{aligned}\sigma_{xy}^{(3)} &= 4e^2 \sum_{\mathbf{k}, i} \left\{ \frac{X(\epsilon)}{\partial_\epsilon D_{\mathbf{k}}} \frac{\delta(\epsilon - \epsilon_i)}{\partial_\epsilon D_{\mathbf{k}}} \right\}_{\epsilon=\mu} \\ &\quad - \int_{-\infty}^{\mu} d\epsilon \left[\frac{\partial}{\partial\epsilon} \left(\frac{X(\epsilon)}{\partial_\epsilon D_{\mathbf{k}}} \right) \right] \frac{\delta(\epsilon - \epsilon_i)}{\partial_\epsilon D_{\mathbf{k}}} \right\}.\end{aligned}\quad (57)$$

(The surface term at $\epsilon = -\infty$ vanishes.) In the typical three cases, the integrals in Eq. (57) can be performed analytically (see Appendices B to D), giving

$$\begin{aligned}\sigma_{xy}^{(3)}(S=0) &= -\text{sign}(\mu) \frac{e^2}{4\pi^2} \sum_{\eta} \eta \Theta_{\eta}(\mu) \sqrt{\mu^2 - (m + \eta M)^2},\end{aligned}\quad (58a)$$

$$\begin{aligned}\sigma_{xy}^{(3)}(M=0) &= -\frac{Se^2}{3\pi^2} - \frac{e^2}{4\pi^2} \sum_{\eta} \eta \Theta_{\eta}(\mu) \sqrt{(|\mu| - \eta S)^2 - m^2},\end{aligned}\quad (58b)$$

$$\begin{aligned}\sigma_{xy}^{(3)}(M=S) &= -\frac{Se^2}{3\pi^2} - \frac{e^2}{12\pi^2} \sum_{\eta} \eta \Theta_{\eta}(\mu) \xi_{\eta} \\ &\quad \times \frac{2 \text{sign}(\mu)(\mu - m - 2\eta S) + \mu + 2m + \eta S}{|\mu - \eta S|},\end{aligned}\quad (58c)$$

for cases (i), (ii) and (iii), respectively.

IV. RESULTS AND DISCUSSION

In this section, we show the results for (i) $(M, S) = (0.4m, 0)$, (ii) $(M, S) = (0, 0.4m)$, and (iii) $(M, S) = (0.2m, 0.2m)$. These parameter sets give the same exchange shift, $\pm(S + M) = \pm 0.4m$, in the upper Dirac band (positive-energy states). Some subtle features present in the Fermi-sea terms (ultraviolet divergence) are also reported.

A. AMR

The longitudinal conductivity for perpendicular ($\sigma_{\perp} = \sigma_{xx} = \sigma_{yy}$) or parallel ($\sigma_{\parallel} = \sigma_{zz}$) configuration, together with the one in the paramagnetic state ($M = S = 0$), are plotted in Fig. 2 as functions of μ . The AMR ratio, $(\sigma_{\perp} - \sigma_{\parallel})/(\sigma_{\perp} + \sigma_{\parallel})$, is plotted in Fig. 3 against the scaled chemical potential, x , defined by

$$\mu = m + (M + S)(x - 1). \quad (59)$$

Note that $x = 0$ ($x = 2$) corresponds to the bottom of the majority- (minority-) spin band in the upper Dirac bands (positive-energy states). As seen, the sign of AMR is opposite between (i) and (ii) and the magnitudes are comparable and large ($5 \sim 25\%$). In contrast, for (iii), the magnitude is much smaller ($0.1 \sim 1\%$). To see the physical origin, we note that the (diagonal) conductivity is written as $\sigma_A = e^2 \langle v_A^2 \tau_{\mathbf{k}} \rangle \nu(\mu)$, where v_A is the group velocity in the direction specified by A ($=\perp, \parallel$), $\tau_{\mathbf{k}}$ is the relaxation time, $\nu(\mu)$ is the density of states at μ , and $\langle \dots \rangle$ represents averaging over the Fermi surfaces. For (iii), since the group velocity is isotropic, the AMR should be ascribed to the anisotropy of $\tau_{\mathbf{k}}$. Note that, although the damping constants in the original representation, given by Eq. (15) [or Eqs. (A5a) to (A5d) for explicit forms], do not depend on \mathbf{k} , the damping of band electrons (obtained after the band diagonalization) depends on \mathbf{k} in general. For (i) and (ii), the two observations made above (magnitude and sign of AMR ratio) indicate that AMR in these cases is totally due to the anisotropy of the band structure (group velocity). (Recall that the deformation of the Fermi surface is opposite between (i) and (ii).)

The above features can already be seen in the weak-relativistic limit.³ The effective Hamiltonian in this case is derived by the Foldy-Wouthuysen-Tani transformation^{28,29} as³⁰

$$\begin{aligned}\mathcal{H}_{\text{Pauli}} &= \frac{k^2}{2m} - (\mathbf{M} + \mathbf{S}) \cdot \boldsymbol{\sigma} + V_{\text{imp}} \\ &\quad + \frac{1}{2m^2} \{ (\mathbf{k} \cdot (\mathbf{M} - \mathbf{S})) (\mathbf{k} \cdot \boldsymbol{\sigma}) + (\mathbf{S} \cdot \boldsymbol{\sigma}) k^2 \} \\ &\quad + \frac{1}{4m^2} (\mathbf{k} \times \nabla V_{\text{imp}}) \cdot \boldsymbol{\sigma}.\end{aligned}\quad (60)$$

The first term in the second line, containing $\mathbf{M} - \mathbf{S}$, introduces anisotropy in the energy dispersion. This anisotropy vanishes for $\mathbf{M} = \mathbf{S}$; in this case, only the conventional SOC due to the impurity potential connects the spin and the direction of \mathbf{k} , and the AMR for case (iii) can be ascribed to this term. The AMR ratio near the region $M = S$ is plotted in Fig. 3 as a function of $M - S$ (and μ) while keeping $M + S$ constant. The second term in the second line, containing $\mathbf{S} \cdot \boldsymbol{\sigma}$, represents spin-dependent effective mass.³¹

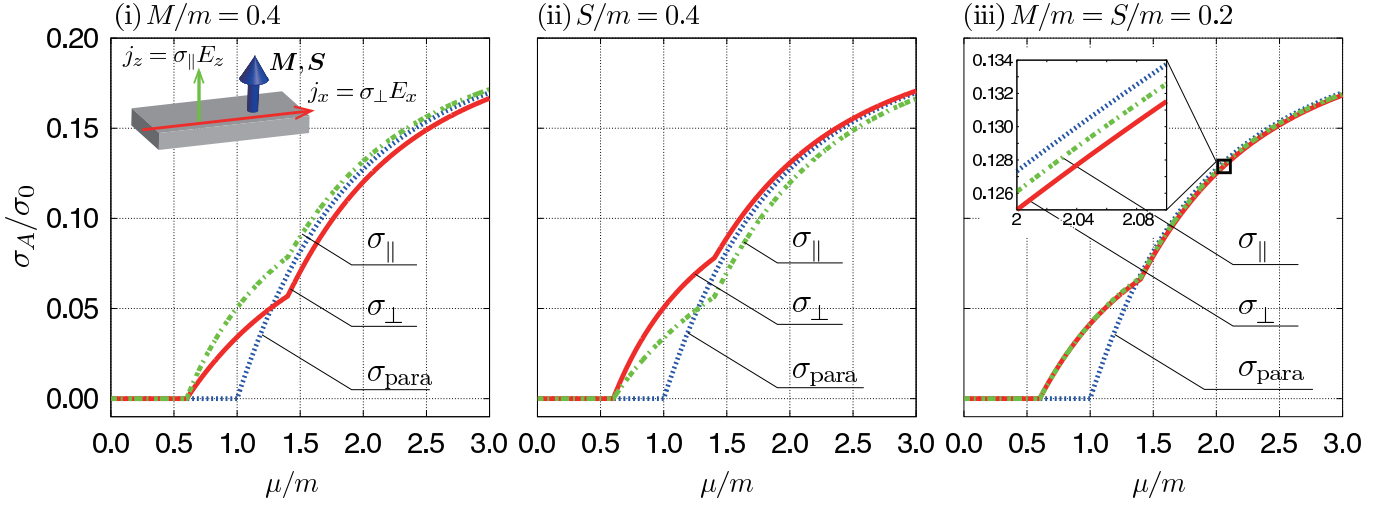


FIG. 2: (Color online) Diagonal conductivity σ_A ($A = \parallel, \perp$) as functions of chemical potential μ for the three typical cases (i)-(iii), normalized by $\sigma_0 = e^2 m^2 c^3 / \hbar^2 \gamma_0$ with $\gamma_0 = n_i u^2 m^2 c / \hbar^3$. Those in the paramagnetic state ($M = S = 0$) are also plotted as σ_{para} . The inset to (i) illustrates mutual directions of \mathbf{M} , \mathbf{S} and $\mathbf{j} = \sigma_A \mathbf{E}$.

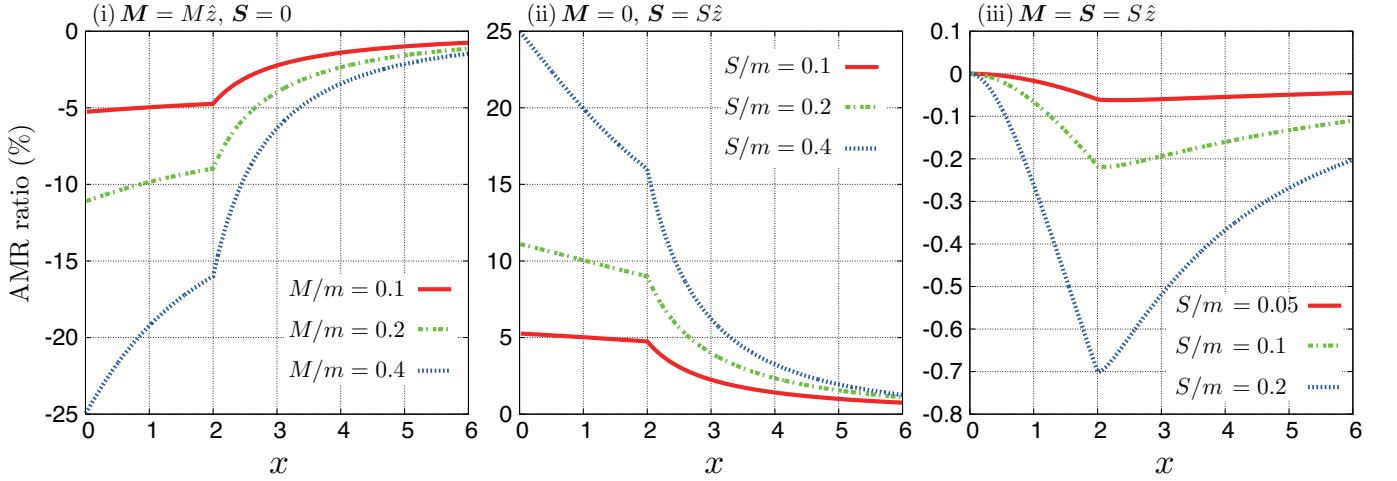


FIG. 3: (Color online) The AMR ratio $(\sigma_{\perp} - \sigma_{\parallel})/(\sigma_{\perp} + \sigma_{\parallel}) \times 100$ plotted against a reduced chemical potential, $x = 1 + (\mu - m)/(M + S)$, defined by Eq. (59). The bottom of the first (second) band in the upper Dirac band (positive-energy state) corresponds to $x = 0$ ($x = 2$).

B. AHE

Figure 5 shows the μ -dependence of σ_{xy} , which consists of the the Fermi-surface term $\sigma_{xy}^{(2)}$ and the Fermi-sea term $\sigma_{xy}^{(3)}$. We see that it is an odd function of μ , $\sigma_{xy}(\mu, M) = -\sigma_{xy}(-\mu, M)$, in case (i), and an even function of μ , $\sigma_{xy}(\mu, S) = \sigma_{xy}(-\mu, S)$, in case (ii). Indeed, one can show that (see Appendix E)

$$\begin{aligned} \sigma_{xy}(\mu, M, S) &= -\sigma_{xy}(-\mu, M, -S) \\ &= \sigma_{xy}(-\mu, -M, S), \end{aligned} \quad (61)$$

from which the above symmetry properties follow if we put $S = 0$ or $M = 0$.

Remarkably, in cases (ii) and (iii), the AH conductivity takes a finite value,

$$\sigma_{xy}(\mu = 0) = -\frac{e^2 S}{3\pi^2 \hbar^2 c} = -\frac{\alpha S}{3\pi^2 \hbar}, \quad (62)$$

even in the insulating state where μ lies in the band gap. Here $\alpha = e^2 / \hbar c$ is the (effective) fine structure constant. This is obtained from Eqs. (58b) and (58c) by dropping the second terms, which vanish in the gap due to $\Theta_{\eta}(\epsilon)$, while in case (i), it vanishes because of the symmetry, $\sigma_{xy}(\mu = 0, M) = -\sigma_{xy}(\mu = 0, M)$. The value is exactly proportional to the “spin” order parameter, S , hence is not quantized. This state thus exemplifies a “non-quantized Hall insulator” in three spatial dimensions.

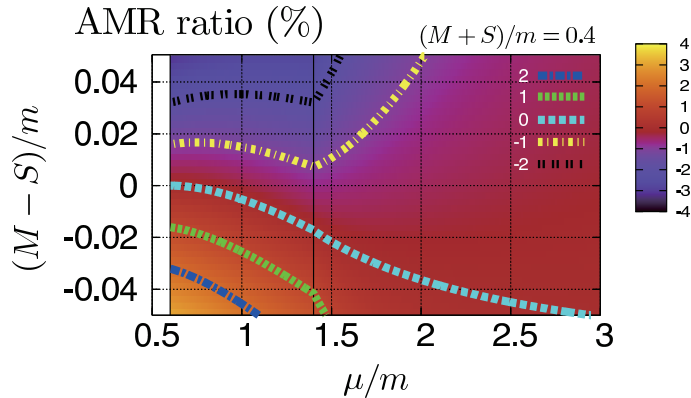


FIG. 4: (Color online) The AMR ratio $(\sigma_{\perp} - \sigma_{\parallel})/(\sigma_{\perp} + \sigma_{\parallel}) \times 100$ plotted in the plane of μ and $M - S$, with $M + S = 0.4m$ kept constant. The white region ($\mu/m < 0.6$) represents the energy gap. There is a single Fermi surface for $0.6 < \mu/m < 1.4$, and are two Fermi surfaces for $\mu/m > 1.4$.

Recently, Samarth *et al.* found that in Cr-doped $(\text{Bi,Sb})_2\text{Te}_3$ the Hall conductivity develops at low temperatures while the resistivity continues to increase down to the lowest temperature.¹⁰ These features seem to be consistent with the above Hall insulator state with a ferromagnetic order parameter given by \mathbf{S} (purely \mathbf{S} , or a mixture of \mathbf{S} and \mathbf{M}).

C. Regularization dependence of Fermi-sea term

In cases (ii) and (iii), the Fermi-sea terms contain ultraviolet divergences and we have managed them by introducing a momentum cut-off Λ and letting $\Lambda \rightarrow \infty$ at the end. The above results, Eq. (62) and first terms in Eqs. (58b) and (58c), were obtained based on the isotropic cut-off, $|\mathbf{k}| < \Lambda$. If other cut-off scheme is used (such as the anisotropic one), one generally obtains a different value. For example, if we take the “elliptical” cut-off,

$$k_{\perp}^2 + (1 + \lambda)k_z^2 \leq \Lambda^2 \quad (-1 < \lambda < \infty), \quad (63)$$

Eq. (62) is replaced by

$$\sigma_{xy}(\mu = 0) = -\frac{\alpha S}{3\pi^2 \hbar} g(\lambda), \quad (64)$$

[so are the first terms of Eqs. (58b) and (58c)], where $g(\lambda)$ is given by Eq. (C20) and plotted in Fig. 6. (See Appendices C and D for details). While the isotropic cut-off seems to be most natural, anisotropic cut-off may find its relevance in real materials having crystal anisotropy.

V. SUMMARY

We have proposed a model ferromagnet based on the Dirac Hamiltonian in 3D by noting that there are two possible ferromagnetic order parameters, \mathbf{M} and \mathbf{S} . By restricting ourselves to the case where \mathbf{M} and \mathbf{S} are collinear, we have studied its magneto-transport properties, which are AMR and AHE. The AMR is found to be determined primarily by the anisotropy of the Fermi surface (group velocity) and secondarily by the anisotropy of the damping. As for AHE, the present model offers an example of non-quantized Hall insulator state in which the Hall conductivity is proportional to \mathbf{S} while the longitudinal conductivity vanishes. We have suggested that this may explain the peculiar property of Cr-doped $(\text{Bi,Sb})_2\text{Te}_3$ found in a recent experiment.¹⁰

In this paper, we have restricted ourselves to the process represented by a simple bubble diagram, in which only the self-energy effects are considered. It will be important to study the effects of vertex corrections such as ladder and skew scattering. These will be reported in the future.

Acknowledgments

The authors would like to thank Prof. N. Samarth for his kind correspondence. This work was supported by Grants-in-Aid for Scientific Research (No. 21540336, No. 24244053 and No. 25400339) from the Japan Society for the Promotion of Science (JSPS). JF is supported by JSPS Research Fellowship for Young Scientists.

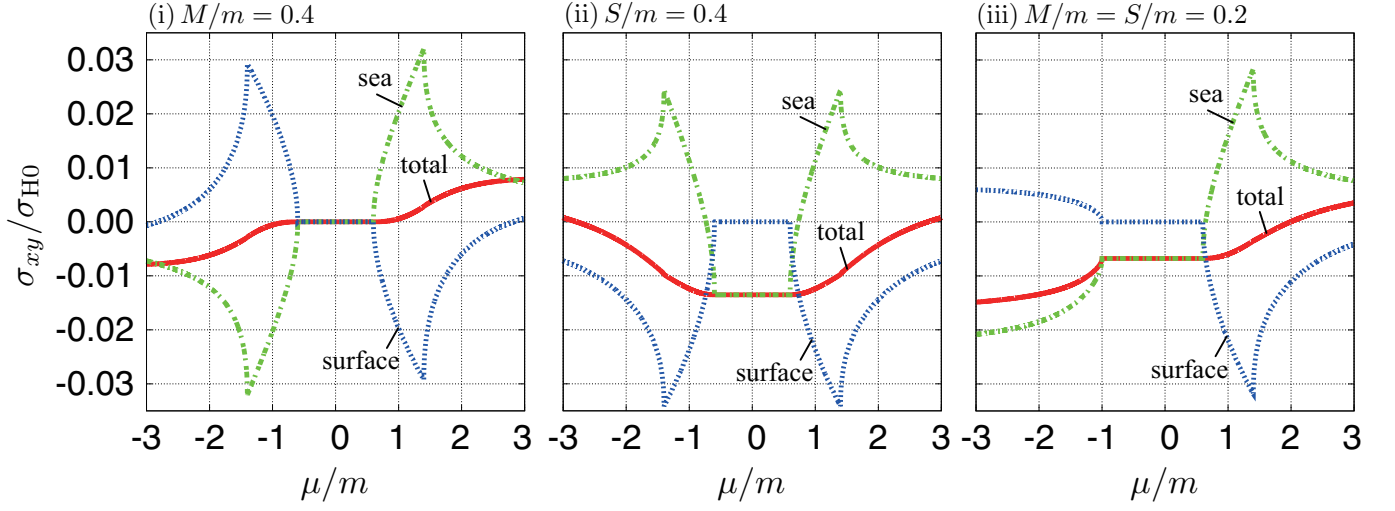


FIG. 5: (Color online) The off-diagonal (Hall) conductivity $\sigma_{xy} = \sigma_{xy}^{(2)} + \sigma_{xy}^{(3)}$ as functions of μ , where $\sigma_{xy}^{(2)}$ is the Fermi-surface term and $\sigma_{xy}^{(3)}$ is the Fermi-sea term, each of which are also shown. They are normalized by $\sigma_{H0} = e^2 mc/\hbar^2$.

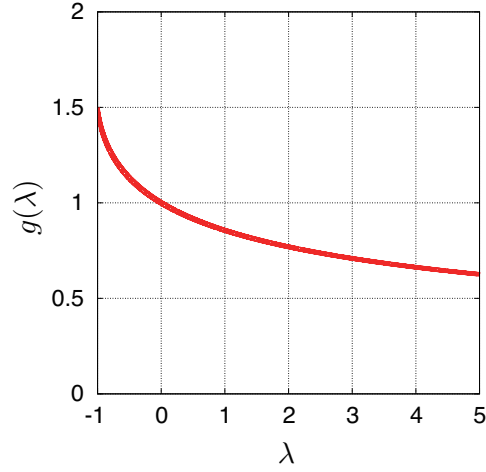


FIG. 6: (Color online) The function $g(\lambda)$ [Eq. (C20)], where λ is the ellipticity parameter of the ultraviolet cut-off [Eq. (63)].

Appendix A: Damping constants

The damping constants $\gamma_{\mu\nu}(\epsilon)$ given by Eq. (15) are calculated as follows. Using the relation

$$\begin{aligned} \text{Im} \frac{1}{D_{\mathbf{k}}(\epsilon + i0)} &= -\frac{\pi}{4\epsilon(\epsilon^2 - \epsilon_k^2)} \sum_{\eta, \zeta} \delta(\epsilon - \zeta \chi_{\mathbf{k}}^{\eta}(\epsilon)) \\ &= -\frac{\pi}{8\epsilon \Delta_{\mathbf{k}}(\epsilon)} \sum_{\eta, \zeta} \eta \delta(\epsilon - \zeta \chi_{\mathbf{k}}^{\eta}(\epsilon)), \end{aligned} \quad (\text{A1})$$

where

$$\chi_{\mathbf{k}}^{\eta}(\epsilon) = \sqrt{\epsilon_k^2 + 2\eta \Delta_{\mathbf{k}}(\epsilon)}, \quad (\text{A2})$$

they are written as

$$\gamma_{00}(\epsilon) = \frac{\pi}{4} n_i u^2 \frac{1}{\epsilon} \sum_{\mathbf{k}, \eta, \zeta} \left\{ \epsilon - \frac{\eta M \Omega}{\Delta_{\mathbf{k}}(\epsilon)} \right\} \delta(\epsilon - \zeta \chi_{\mathbf{k}}^{\eta}(\epsilon)), \quad (\text{A3a})$$

$$\gamma_{30}(\epsilon) = \frac{\pi}{4} n_i u^2 \frac{1}{\epsilon} \sum_{\mathbf{k}, \eta, \zeta} \left\{ m + \frac{\eta S \Omega}{\Delta_{\mathbf{k}}(\epsilon)} \right\} \delta(\epsilon - \zeta \chi_{\mathbf{k}}^{\eta}(\epsilon)), \quad (\text{A3b})$$

$$\gamma_{0z}(\epsilon) = -\frac{\pi}{4} n_i u^2 \frac{1}{\epsilon} \sum_{\mathbf{k}, \eta, \zeta} \left\{ S + \frac{\eta S k_z^2}{\Delta_{\mathbf{k}}(\epsilon)} + \frac{\eta m \Omega}{\Delta_{\mathbf{k}}(\epsilon)} \right\} \delta(\epsilon - \zeta \chi_{\mathbf{k}}^{\eta}(\epsilon)), \quad (\text{A3c})$$

$$\gamma_{3z}(\epsilon) = \frac{\pi}{4} n_i u^2 \frac{1}{\epsilon} \sum_{\mathbf{k}, \eta, \zeta} \left\{ M + \frac{\eta M k_z^2}{\Delta_{\mathbf{k}}(\epsilon)} - \frac{\eta \epsilon \Omega}{\Delta_{\mathbf{k}}(\epsilon)} \right\} \delta(\epsilon - \zeta \chi_{\mathbf{k}}^{\eta}(\epsilon)). \quad (\text{A3d})$$

If we define

$$\nu_{l,m}^{\eta}(\epsilon) = \sum_{\mathbf{k}, \zeta} \frac{k_z^{2m}}{[\Delta_{\mathbf{k}}(\epsilon)]^l} \delta(\epsilon - \zeta \chi_{\mathbf{k}}^{\eta}(\epsilon)), \quad (\text{A4})$$

the $\gamma_{\mu\nu}(\epsilon)$'s are expressed as

$$\gamma_{00}(\epsilon) = \frac{\pi}{4} n_i u^2 \frac{1}{\epsilon} \sum_{\eta} (\epsilon \nu_{0,0}^{\eta}(\epsilon) - \eta M \Omega \nu_{1,0}^{\eta}(\epsilon)), \quad (\text{A5a})$$

$$\gamma_{30}(\epsilon) = \frac{\pi}{4} n_i u^2 \frac{1}{\epsilon} \sum_{\eta} (m \nu_{0,0}^{\eta}(\epsilon) + \eta S \Omega \nu_{1,0}^{\eta}(\epsilon)), \quad (\text{A5b})$$

$$\gamma_{0z}(\epsilon) = -\frac{\pi}{4} n_i u^2 \frac{1}{\epsilon} \sum_{\eta} (S \nu_{0,0}^{\eta}(\epsilon) + \eta S \nu_{1,1}^{\eta}(\epsilon) + \eta m \Omega \nu_{1,0}^{\eta}(\epsilon)), \quad (\text{A5c})$$

$$\gamma_{3z}(\epsilon) = \frac{\pi}{4} n_i u^2 \frac{1}{\epsilon} \sum_{\eta} (M \nu_{0,0}^{\eta}(\epsilon) + \eta M \nu_{1,1}^{\eta}(\epsilon) - \eta \epsilon \Omega \nu_{1,0}^{\eta}(\epsilon)). \quad (\text{A5d})$$

For $(l, m) = (0, 0), (1, 0), (1, 1)$, they are calculated as

$$\nu_{0,0}^{\eta}(\epsilon) = \frac{|\epsilon|}{2\pi^2} \Theta_{\eta}(\epsilon) \xi_{\eta}(\epsilon), \quad (\text{A6})$$

$$\nu_{1,0}^{\eta}(\epsilon) = \frac{|\epsilon|}{2\pi^2} \Theta_{\eta}(\epsilon) h_{\eta}(\epsilon), \quad (\text{A7})$$

$$\nu_{1,1}^{\eta}(\epsilon) = \frac{|\epsilon|}{4\pi^2} \Theta_{\eta}(\epsilon) \frac{1}{S^2 - M^2} \left(\xi_{\eta}(\epsilon) \sqrt{\Omega^2 + (S^2 - M^2)[\xi_{\eta}(\epsilon)]^2} - \Omega^2 h_{\eta}(\epsilon) \right), \quad (\text{A8})$$

where

$$h_{\eta}(\epsilon) = \begin{cases} \frac{1}{\sqrt{S^2 - M^2}} \tanh^{-1} \frac{\xi_{\eta}(\epsilon) \sqrt{S^2 - M^2}}{\sqrt{\Omega^2 + (S^2 - M^2)[\xi_{\eta}(\epsilon)]^2}} & (S^2 - M^2 > 0), \\ \frac{1}{\sqrt{|S^2 - M^2|}} \tan^{-1} \frac{\xi_{\eta}(\epsilon) \sqrt{|S^2 - M^2|}}{\sqrt{\Omega^2 - |S^2 - M^2|[\xi_{\eta}(\epsilon)]^2}} & (S^2 - M^2 < 0), \end{cases} \quad (\text{A9})$$

and $\xi_{\eta}(\epsilon)$ and $\Theta_{\eta}(\epsilon)$ are defined by Eqs. (42) and (47), respectively.

Appendix B: “Magnetization” model

In this Appendix, we show some details of the calculation for the “magnetization” model, in which $\mathbf{M} = M\hat{z}$ and $\mathbf{S} = 0$ [case (i)]. The denominator, $D_{\mathbf{k}}(\epsilon)$, of the unperturbed Green's function is given by

$$D_{\mathbf{k}}(\epsilon) = (\epsilon - E_{\mathbf{k}}^+)(\epsilon + E_{\mathbf{k}}^+)(\epsilon - E_{\mathbf{k}}^-)(\epsilon + E_{\mathbf{k}}^-), \quad (\text{B1})$$

$$E_{\mathbf{k}}^{\eta} = \sqrt{k^2 + m^2 + M^2 + 2\eta M \sqrt{k_{\perp}^2 + m^2}} \quad (\text{B2})$$

$$= \sqrt{\epsilon_k^2 + 2M^2 + 2\eta M \sqrt{k_{\perp}^2 + m^2}}, \quad (\text{B3})$$

where $\eta = \pm$, $k_{\perp}^2 = k_x^2 + k_y^2$, and $\epsilon_k^2 = k^2 + m^2 - M^2$.

It is convenient to define the generalized density of states by

$$\mathcal{N}_{l,\eta}(\epsilon) = \sum_{\mathbf{k}} \sum_{\zeta=\pm 1} (k_{\perp}^2 + m^2)^{l/2} \delta(\epsilon - \zeta E_{\mathbf{k}}^{\eta}). \quad (\text{B4})$$

Using the relation $\sum_{\zeta} \delta(\epsilon - \zeta E_{\mathbf{k}}^{\eta}) = 2|\epsilon| \delta(k_z^2 - \epsilon^2 + (\sqrt{k_{\perp}^2 + m^2} + \eta M)^2)$ and performing the \mathbf{k} -integration, those of our interest (see below) are obtained as

$$\mathcal{N}_{-1,\eta}(\epsilon) = \frac{|\epsilon|}{2\pi^2} \Theta_{\eta}(\epsilon) \left(\frac{\pi}{2} - \psi_a \right), \quad (\text{B5})$$

$$\mathcal{N}_{0,\eta}(\epsilon) = \frac{|\epsilon|}{2\pi^2} \Theta_{\eta}(\epsilon) \left(|\epsilon| \cos \psi_a - \eta M \left(\frac{\pi}{2} - \psi_a \right) \right), \quad (\text{B6})$$

$$\mathcal{N}_{1,\eta}(\epsilon) = \frac{|\epsilon|}{4\pi^2} \Theta_{\eta}(\epsilon) \left((m - 3\eta M) |\epsilon| \cos \psi_a + (\epsilon^2 + 2M^2) \left(\frac{\pi}{2} - \psi_a \right) \right), \quad (\text{B7})$$

where $\psi_a = \sin^{-1}[(m + \eta M)/|\epsilon|]$, and

$$\Theta_{\eta}(\epsilon) = \begin{cases} 1 & (|\epsilon| > m + \eta M) \\ 0 & (\text{otherwise}). \end{cases} \quad (\text{B8})$$

To calculate $\sigma_{xy}^{(3)}$, we note $X(\epsilon) = -4mM\epsilon(\epsilon^2 - \epsilon_k^2)$ [Eq. (56)] and $\partial_{\epsilon} D_{\mathbf{k}} = 4\epsilon(\epsilon^2 - \epsilon_k^2 - 2M^2)$, and rewrite Eq. (57) as

$$\sigma_{xy}^{(3)} = -\frac{me^2}{2\mu} \sum_{\eta} (\eta \mathcal{N}_{-1,\eta}(\mu) + M \mathcal{N}_{-2,\eta}(\mu)) - \frac{me^2}{2} \sum_{\eta} \eta \sum_{\mathbf{k},\zeta} \frac{1}{(k_{\perp}^2 + m^2)^{3/2}} \int_{-\infty}^{\mu} d\epsilon \delta(\epsilon - \zeta E_{\mathbf{k}}^{\eta}). \quad (\text{B9})$$

In the second term on the right-hand side, the ϵ -integral in the range $(-\infty, 0)$ vanishes because of $\sum_{\eta} \eta = 0$, and the rest of the ϵ - and \mathbf{k} -integrals are calculated as follows:

$$\begin{aligned} \sum_{\mathbf{k},\zeta} \frac{1}{(k_{\perp}^2 + m^2)^{3/2}} \int_0^{\mu} d\epsilon \delta(\epsilon - \zeta E_{\mathbf{k}}^{\eta}) &= \frac{1}{(2\pi)^2} \Theta_{\eta}(\mu) \int_0^{\xi_{\eta}} dk_{\perp} \frac{2k_{\perp}}{(k_{\perp}^2 + m^2)^{3/2}} \int_0^{\sqrt{\mu^2 - (\sqrt{k_{\perp}^2 + m^2} + \eta M)^2}} dk_z \\ &= \frac{\mu|\mu|}{2\pi^2} \Theta_{\eta}(\mu) \int_{\psi_a}^{\psi_b} d\theta \frac{\cos^2 \theta}{(\mu \sin \theta - \eta M)^2} \\ &= \frac{|\mu|}{2\pi^2} \Theta_{\eta}(\mu) \left[\frac{1}{m} \cos \psi_a - \frac{1}{\mu} \int_{\psi_a}^{\psi_b} d\theta \left(1 + \frac{\eta M}{\mu \sin \theta - \eta M} \right) \right] \\ &= \frac{1}{m\mu} (\mathcal{N}_{0,\eta}(\mu) + \eta M \mathcal{N}_{-1,\eta}(\mu)) - \frac{1}{\mu} (\mathcal{N}_{-1,\eta}(\mu) + \eta M \mathcal{N}_{-2,\eta}(\mu)). \end{aligned} \quad (\text{B10})$$

Therefore, the second term in Eq. (B9) can be rewritten as

$$-\frac{e^2}{2\mu} \sum_{\eta} [(\eta \mathcal{N}_{0,\eta}(\mu) + M \mathcal{N}_{-1,\eta}(\mu)) - m(\eta \mathcal{N}_{-1,\eta}(\mu) + M \mathcal{N}_{-2,\eta}(\mu))], \quad (\text{B11})$$

and we obtain

$$\begin{aligned} \sigma_{xy}^{(3)} &= -\frac{e^2}{2\mu} \sum_{\eta} (\eta \mathcal{N}_{0,\eta}(\mu) + M \mathcal{N}_{-1,\eta}(\mu)) \\ &= -\text{sign}(\mu) \frac{e^2}{4\pi^2} \sum_{\eta} \eta \Theta_{\eta}(\mu) \sqrt{\mu^2 - (m + \eta M)^2}. \end{aligned} \quad (\text{B12})$$

These are shown in Fig. 5 (i) as the Fermi-sea term.

Appendix C: “Spin” model

For the “spin” model, where $\mathbf{M} = 0$ and $\mathbf{S} = S\hat{z}$ [case (ii)], the denominator $D_{\mathbf{k}}(\epsilon)$ [Eq. (9)] of the unperturbed Green’s function is given by

$$D_{\mathbf{k}}(\epsilon) = (\epsilon - E_{\mathbf{k}}^+)(\epsilon + E_{\mathbf{k}}^+)(\epsilon - E_{\mathbf{k}}^-)(\epsilon + E_{\mathbf{k}}^-), \quad (\text{C1})$$

$$E_{\mathbf{k}}^\eta = \sqrt{k^2 + m^2 + S^2 + 2\eta S\sqrt{k_z^2 + m^2}} \quad (\text{C2})$$

$$= \sqrt{\epsilon_k^2 + 2\eta S\sqrt{k_z^2 + m^2}}, \quad (\text{C3})$$

where $\epsilon_k^2 = k^2 + m^2 + S^2$.

The generalized density of states in this case is defined by

$$\mathcal{N}_{l,\eta}(\epsilon) = \sum_{\mathbf{k},\zeta} (k_z^2 + m^2)^{l/2} \delta(\epsilon - \zeta E_{\mathbf{k}}^\eta), \quad (\text{C4})$$

some of which are calculated as

$$\mathcal{N}_{-1,\eta}(\epsilon) = \frac{|\epsilon|}{2\pi^2} \theta_\eta^*(\epsilon) \Theta_\eta(\epsilon), \quad (\text{C5})$$

$$\mathcal{N}_{0,\eta}(\epsilon) = \frac{m|\epsilon|}{2\pi^2} \sinh \theta_\eta^*(\epsilon) \Theta_\eta(\epsilon), \quad (\text{C6})$$

$$\mathcal{N}_{1,\eta}(\epsilon) = \frac{m^2|\epsilon|}{4\pi^2} (\theta_\eta^* + \sinh \theta_\eta^*(\epsilon) \cosh \theta_\eta^*(\epsilon)) \Theta_\eta(\epsilon), \quad (\text{C7})$$

where $\theta_\eta^*(\epsilon) = \cosh^{-1}[(|\epsilon| - \eta S)/m]$ and

$$\Theta_\eta(\epsilon) = \begin{cases} 1 & (|\epsilon| > m + \eta S) \\ 0 & (\text{otherwise}). \end{cases} \quad (\text{C8})$$

To calculate $\sigma_{xy}^{(3)}$, we first express it as

$$\sigma_{xy}^{(3)} = -\frac{e^2}{2\mu^2} \sum_{\eta} (S\mathcal{N}_{0,\eta}(\mu) + \eta\mathcal{N}_{1,\eta}(\mu)) - \frac{e^2}{2} \sum_{\mathbf{k},\eta,\zeta} \eta \frac{\sqrt{k_z^2 + m^2} + \eta S}{\zeta (E_{\mathbf{k}}^\eta)^3} \int_{-\infty}^{\mu} d\epsilon \delta(\epsilon - \zeta E_{\mathbf{k}}^\eta), \quad (\text{C9})$$

by noting that $X(\epsilon) = -S\{D_k + 4(k_z^2 + m^2)(\epsilon^2 - \epsilon_k^2 + 2S^2)\}$ and $\partial_\epsilon D_k = 4\epsilon(\epsilon^2 - \epsilon_k^2)$. In the second term on the right-hand side, the ϵ -integral in the range $(-\infty, 0)$ is calculated as

$$-\frac{e^2}{2} \sum_{\mathbf{k},\eta,\zeta} \eta \frac{\sqrt{k_z^2 + m^2} + \eta S}{\zeta (E_{\mathbf{k}}^\eta)^3} \int_{-\infty}^0 d\epsilon \delta(\epsilon - \zeta E_{\mathbf{k}}^\eta) = \frac{e^2}{2} \sum_{\mathbf{k},\eta} \frac{S + \eta\sqrt{k_z^2 + m^2}}{(E_{\mathbf{k}}^\eta)^3}. \quad (\text{C10})$$

In calculating this \mathbf{k} -integral, a care is needed since it is ultraviolet divergent. To manage this divergence, we introduce a momentum cut-off Λ and limit the integration to a spherical region, $|\mathbf{k}| < \Lambda$, and then let $\Lambda \rightarrow \infty$. This proceeds as follows; we first write

$$\begin{aligned} & \frac{e^2}{2(2\pi)^2} \lim_{\Lambda \rightarrow \infty} \sum_{\eta} \int_0^\Lambda dk_z (S + \eta\sqrt{k_z^2 + m^2}) \int_0^{\sqrt{\Lambda^2 - k_z^2}} dk_\perp 2k_\perp \left(\frac{1}{k_\perp^2 + (S + \eta\sqrt{k_z^2 + m^2})^2} \right)^{3/2} \\ &= -\frac{e^2}{(2\pi)^2} \lim_{\Lambda \rightarrow \infty} \sum_{\eta} \int_0^\Lambda dk_z \frac{S + \eta\sqrt{k_z^2 + m^2}}{\sqrt{\Lambda^2 - k_z^2 + (S + \eta\sqrt{k_z^2 + m^2})^2}}, \end{aligned} \quad (\text{C11})$$

then scale as $k_z = \Lambda t$, $\tilde{m} = m/\Lambda$, $\tilde{S} = S/\Lambda$, and sum over η . The result is the left-hand side of

$$-\frac{Se^2}{(2\pi)^2} \lim_{\Lambda \rightarrow \infty} \int_0^1 dt \{ \mathcal{A}(t) - 4\mathcal{B}(t) \} = -\frac{Se^2}{3\pi^2}, \quad (\text{C12})$$

with

$$\mathcal{A}(t) = \sum_{\eta} \left\{ 1 - t^2 + \left(\tilde{S} + \eta \sqrt{t^2 + \tilde{m}^2} \right)^2 \right\}^{-1/2}, \quad (\text{C13})$$

$$\mathcal{B}(t) = \frac{t^2 + \tilde{m}^2}{\sum_{\eta} \left\{ 1 - t^2 + \left(\tilde{S} + \eta \sqrt{t^2 + \tilde{m}^2} \right)^2 \right\}^{1/2} \prod_{\eta'} \left\{ 1 - t^2 + \left(\tilde{S} + \eta' \sqrt{t^2 + \tilde{m}^2} \right)^2 \right\}^{1/2}}. \quad (\text{C14})$$

We then let $\Lambda \rightarrow \infty$, thus $\tilde{S} \rightarrow 0$, $\tilde{m} \rightarrow 0$, $\mathcal{A} \rightarrow 2$ and $\mathcal{B} \rightarrow t^2/2$, and integrate over t ; this leads to the right-hand side of Eq. (C12). The rest of the integral, which is divergence-free, is calculated as follows,

$$\begin{aligned} & -\frac{e^2}{2(2\pi)^2} \sum_{\eta} \Theta_{\eta}(\mu) \int_0^{\xi_{\eta}} dk_z (S + \eta \sqrt{k_z^2 + m^2}) \int_0^{\alpha_{\eta}} dt \left(\frac{1}{t + (S + \eta \sqrt{k_z^2 + m^2})^2} \right)^{3/2} \\ &= \frac{e^2}{2|\mu|} \frac{1}{2\pi^2} \sum_{\eta} \Theta_{\eta}(\mu) \int_0^{\xi_{\eta}} dk_z (S - \eta|\mu| + \eta \sqrt{k_z^2 + m^2}) \\ &= \frac{e^2}{2|\mu|} \frac{1}{2\pi^2} \sum_{\eta} \Theta_{\eta}(\mu) \int_0^{\theta_{\eta}^*} d\theta m \cosh \theta (S - \eta|\mu| + \eta m \cosh \theta) \\ &= \frac{e^2}{2\mu^2} \sum_{\eta} \{ (S - \eta|\mu|) \mathcal{N}_{0,\eta}(\mu) + \eta \mathcal{N}_{1,\eta}(\mu) \}. \end{aligned} \quad (\text{C15})$$

Therefore we obtain

$$\begin{aligned} \sigma_{xy}^{(3)} &= -\frac{Se^2}{3\pi^2} - \frac{e^2}{2|\mu|} \sum_{\eta} \eta \mathcal{N}_{0,\eta}(\mu) \\ &= -\frac{Se^2}{3\pi^2} - \frac{e^2}{4\pi^2} \sum_{\eta} \eta \Theta_{\eta}(\mu) \sqrt{(|\mu| - \eta S)^2 - m^2}. \end{aligned} \quad (\text{C16})$$

This is plotted in Fig. 5 (ii) as the Fermi-sea term. The first term corresponds to $\sigma_{xy}(\mu = 0)$.

It should be noted that, if another cut-off scheme is adopted, one would obtain a different result in general. For example, if we introduce two cut-off parameters, Λ_{\perp} and Λ_z , limit the integration to a cylindrical region, $|\mathbf{k}_{\perp}| < \Lambda_{\perp}$ and $|k_z| < \Lambda_z$, and let $\Lambda_{\perp} \rightarrow \infty$ and $\Lambda_z \rightarrow \infty$ by keeping the ratio $\Lambda_{\perp}/\Lambda_z \equiv r$ constant, the first term of Eq. (C16) is replaced by

$$\sigma_{xy}(\mu = 0) = -\frac{Se^2}{2\pi^2 \sqrt{r^2 + 1}}. \quad (\text{C17})$$

Another, probably more natural cut-off which allows anisotropy would be an “elliptical” cut-off [Eq. (63)],

$$k_{\perp}^2 + (1 + \lambda)k_z^2 \leq \Lambda^2, \quad (-1 < \lambda < \infty). \quad (\text{C18})$$

In this case, the first term of Eq. (C16) is replaced by

$$\sigma_{xy}(\mu = 0) = -\frac{Se^2}{3\pi^2} g(\lambda), \quad (\text{C19})$$

where

$$g(\lambda) = \begin{cases} \frac{3}{2\lambda} \left[(1 + \lambda) \frac{\tanh^{-1} \sqrt{-\lambda}}{\sqrt{-\lambda}} - 1 \right] & (-1 < \lambda < 0), \\ \frac{3}{2\lambda} \left[(1 + \lambda) \frac{\tan^{-1} \sqrt{\lambda}}{\sqrt{\lambda}} - 1 \right] & (\lambda > 0), \end{cases} \quad (\text{C20})$$

which is plotted in Fig. 6. The value $g(-1) = 3/2$ at $\lambda = -1$ is consistent with Eq. (C17) with $r = 0$.

Appendix D: “Coexistent” Model

For the “coexistent” model with $\mathbf{M} = \mathbf{S} = S\hat{z}$ [case (iii)], the denominator $D_{\mathbf{k}}(\epsilon)$ [Eq. (9)] of the Green’s function is given by

$$D_{\mathbf{k}}(\epsilon) = (\epsilon - S - E_{\mathbf{k}}^+)(\epsilon + S - E_{\mathbf{k}}^+)(\epsilon - S + E_{\mathbf{k}}^-)(\epsilon + S + E_{\mathbf{k}}^-) \quad (\text{D1})$$

$$= \prod_{\eta, \zeta = \pm} (\epsilon - \eta S - \zeta E_{\mathbf{k}}^\eta), \quad (\text{D2})$$

$$E_{\mathbf{k}}^\eta = \sqrt{k^2 + (m + \eta S)^2}. \quad (\text{D3})$$

In this case, the electron dispersion $\epsilon = \eta S + \zeta E_{\mathbf{k}}^\eta$ is isotropic but there is a loss of particle-hole symmetry, in contrast to the cases (i) and (ii).

The generalized density of states is defined by

$$\begin{aligned} \mathcal{N}_{n,l}^\eta(\epsilon) &\equiv \sum_{\mathbf{k}} \sum_{\zeta} \frac{(k_{\perp}^2 - k_z^2)^l}{(\epsilon^2 - \epsilon_{\mathbf{k}}^2)^n} \delta(\epsilon - \eta S - \zeta E_{\mathbf{k}}^\eta) \\ &= \sum_{\mathbf{k}} \sum_{\zeta} \frac{(k^2/3)^l}{(\epsilon^2 - \epsilon_{\mathbf{k}}^2)^n} \delta(\epsilon - \eta S - \zeta E_{\mathbf{k}}^\eta), \quad (l = 0, 1). \end{aligned} \quad (\text{D4})$$

In the second equality, which holds for $l = 0$ and 1 , we have noted that the energy dispersion is isotropic. Explicitly, they are evaluated as

$$\mathcal{N}_{n,l}^\eta(\epsilon) = \frac{1}{2\pi^2} \frac{1}{3^l} \frac{|\epsilon - \eta S|}{\{2\eta S(\epsilon + m)\}^n} \xi_\eta^{2l+1} \Theta_\eta(\epsilon), \quad (l = 0, 1), \quad (\text{D5})$$

with $\xi_\eta = \sqrt{(\epsilon + m)(\epsilon - m - 2\eta S)}$ and

$$\Theta_\eta(\epsilon) = \begin{cases} 1 & (\epsilon < -m, \epsilon > m + 2\eta S) \\ 0 & (\text{otherwise}). \end{cases} \quad (\text{D6})$$

To calculate $\sigma_{xy}^{(3)}$, we note $X(\epsilon) = SD_{\mathbf{k}} - 2S(\epsilon^2 - \epsilon_{\mathbf{k}}^2)\{(\epsilon + m)^2 - k^2 + 2k_z^2\}$ and $\partial_\epsilon D_{\mathbf{k}} = 4\{\epsilon(\epsilon^2 - \epsilon_{\mathbf{k}}^2) - 2S^2(\epsilon + m)\}$, and express it as

$$\begin{aligned} \sigma_{xy}^{(3)} &= -\frac{e^2}{6} \sum_{\eta} \frac{\mu + 2m + \eta S}{(\mu - \eta S)^2} \eta \mathcal{N}_{0,0}^\eta(\mu) \\ &\quad - \frac{e^2}{2} \sum_{\mathbf{k}, \eta, \zeta} \frac{\eta}{k^2} \left[(m + \eta S) \frac{(k_{\perp}^2 - 2k_z^2)}{(\zeta E_{\mathbf{k}}^\eta)^3} - \frac{2k_z^2}{k^2} \left(\frac{m + \eta S}{\zeta E_{\mathbf{k}}^\eta} \right)^3 + \frac{2k_z^2}{k^2} \right] \int_{-\infty}^{\mu} d\epsilon \delta(\epsilon - \eta S - \zeta E_{\mathbf{k}}^\eta), \end{aligned} \quad (\text{D7})$$

where we used

$$\partial_\epsilon D_{\mathbf{k}} = 8\eta \zeta S E_{\mathbf{k}}^\eta (\epsilon + m), \quad (\text{D8})$$

$$\epsilon^2 - \epsilon_{\mathbf{k}}^2 = 2\eta S(\epsilon + m), \quad (\text{D9})$$

$$\frac{1}{\epsilon + m} = -\frac{1}{k^2} (\epsilon + m - 2\zeta E_{\mathbf{k}}^\eta), \quad (\text{D10})$$

which hold under the presence of $\delta(\epsilon - \eta S - \zeta E_{\mathbf{k}}^\eta)$. In the second term on the right-hand side of Eq. (D7), the ϵ -integral from the range $(-\infty, 0)$ is divided into the convergent part (\mathcal{W}_0) and the conditionally-convergent part (\mathcal{W}_1) due to ultraviolet divergence. They are respectively evaluated as follows; For \mathcal{W}_0 ,

$$\begin{aligned} \mathcal{W}_0 &\equiv -\frac{e^2}{2} \sum_{\mathbf{k}, \eta, \zeta} \frac{\eta}{k^2} \left[-\frac{2k_z^2}{k^2} \left(\frac{m + \eta S}{\zeta E_{\mathbf{k}}^\eta} \right)^3 + \frac{2k_z^2}{k^2} \right] \int_{-\infty}^0 d\epsilon \delta(\epsilon - \eta S - \zeta E_{\mathbf{k}}^\eta) \\ &= -\frac{e^2}{3} \sum_{\mathbf{k}, \eta} \frac{\eta}{k^2} \frac{(m + \eta S)^3}{(E_{\mathbf{k}}^\eta)^3} \\ &= -\frac{e^2}{3} \frac{1}{2\pi^2} \sum_{\eta} \int_0^\infty dk \frac{(m + \eta S)^3}{(E_{\mathbf{k}}^\eta)^3} \\ &= -\frac{Se^2}{3\pi^2}. \end{aligned} \quad (\text{D11})$$

For \mathcal{W}_1 , we introduce a cut-off as $k_\perp^2 + (1 + \lambda)k_z^2 \leq \Lambda^2$ [Eq. (63) or Eq. (C18)], and evaluate as

$$\begin{aligned}\mathcal{W}_1 &\equiv -\frac{e^2}{2} \sum_{\mathbf{k}, \eta, \zeta} \frac{\eta \zeta}{(E_k^\eta)^3} \frac{1}{k^2} (m + \eta S) (k_\perp^2 - 2k_z^2) \int_{-\infty}^0 d\epsilon \delta(\epsilon - \eta S - \zeta E_k^\eta) \\ &= \lim_{\Lambda \rightarrow \infty} \frac{e^2}{2(2\pi)^2} \sum_{\eta} \eta (m + \eta S) \int_0^{1/\sqrt{1+\lambda}} dq \int_{q^2}^{1-\lambda q^2} dp \frac{1}{(p + \epsilon_\eta^2)^{3/2}} \frac{p - 3q^2}{p} \\ &= - \lim_{\epsilon_\eta \rightarrow 0} \frac{e^2}{(2\pi)^2} \sum_{\eta} \eta (m + \eta S) \left(\mathcal{C}_\eta(\lambda) + \mathcal{D}_\eta(\lambda) \right),\end{aligned}\tag{D12}$$

where we put $k_\perp^2 = \Lambda^2(p - q^2)$, $k_z = \Lambda q$, $\epsilon_\eta = (m + \eta S)/\Lambda$, and

$$\mathcal{C}_\eta(\lambda) = \int_0^{1/\sqrt{1+\lambda}} dq \left(\frac{1}{\sqrt{1 - \lambda q^2 + \epsilon_\eta^2}} \left(1 + \frac{3q^2}{\epsilon_\eta^2} \right) - \frac{3q^2}{2\epsilon_\eta^3} \log \frac{\sqrt{1 - \lambda q^2 + \epsilon_\eta^2} + \epsilon_\eta}{\sqrt{1 - \lambda q^2 + \epsilon_\eta^2} - \epsilon_\eta} \right),\tag{D13}$$

$$\mathcal{D}_\eta(\lambda) = \int_0^{1/\sqrt{1+\lambda}} dq \left(\frac{3q^2}{2\epsilon_\eta^3} \log \frac{\sqrt{q^2 + \epsilon_\eta^2} + \epsilon_\eta}{\sqrt{q^2 + \epsilon_\eta^2} - \epsilon_\eta} - \frac{1}{\sqrt{q^2 + \epsilon_\eta^2}} \left(1 + \frac{3q^2}{\epsilon_\eta^2} \right) \right).\tag{D14}$$

The q -integration and the limit $\epsilon_\eta \rightarrow 0$ are mutually commutative in $\mathcal{C}_\eta(\lambda)$, hence we can take the limit $\epsilon_\eta \rightarrow 0$ first,

$$\lim_{\epsilon_\eta \rightarrow 0} \mathcal{C}_\eta(\lambda) = \int_0^{1/\sqrt{1+\lambda}} dq \frac{1}{\sqrt{1 - \lambda q^2}} \left(1 - \frac{q^2}{1 - \lambda q^2} \right) = \frac{2}{3} g(\lambda),\tag{D15}$$

where $g(\lambda)$ is given by Eq. (C20). For $\mathcal{D}_\eta(\lambda)$, they do not commute and we have to perform the q -integral first and then take the limit $\epsilon_\eta \rightarrow 0$,

$$\begin{aligned}\lim_{\epsilon_\eta \rightarrow 0} \mathcal{D}_\eta(\lambda) &= \lim_{\epsilon_\eta \rightarrow 0} \int_0^{1/\sqrt{1+\lambda}} dq \left(\frac{3q^2}{\epsilon_\eta^3} \log \frac{\sqrt{q^2 + \epsilon_\eta^2} + \epsilon_\eta}{q} - \frac{3}{\epsilon_\eta^2} \sqrt{q^2 + \epsilon_\eta^2} + \frac{2}{\sqrt{q^2 + \epsilon_\eta^2}} \right) \\ &= \lim_{\epsilon_\eta \rightarrow 0} \left[\frac{1}{2\epsilon_\eta^3} \left\{ q\epsilon_\eta \sqrt{q^2 + \epsilon_\eta^2} + 2q^3 \log \frac{\sqrt{q^2 + \epsilon_\eta^2} + \epsilon_\eta}{q} - \epsilon_\eta^3 \log(q + \sqrt{q^2 + \epsilon_\eta^2}) \right\} \right. \\ &\quad \left. - \frac{3}{2\epsilon_\eta^2} \left\{ q\sqrt{q^2 + \epsilon_\eta^2} + \epsilon_\eta^2 \log(q + \sqrt{q^2 + \epsilon_\eta^2}) \right\} + 2 \log(q + \sqrt{q^2 + \epsilon_\eta^2}) \right]_{q=0}^{q=1/\sqrt{1+\lambda}} \\ &= -\frac{2}{3}.\end{aligned}\tag{D16}$$

Consequently, we obtain $\mathcal{W}_1 = -(Se^2/3\pi^2)(g(\lambda) - 1)$. Note that $\mathcal{W}_1(\lambda = 0) = 0$ for the isotropic cut-off, $k^2 < \Lambda$. For the rest part of the ϵ -integral of Eq. (D7), since there is no divergence and the dispersion is isotropic, we evaluate it by replacing k_\perp^2 by $2k^2/3$ and k_z^2 by $k^2/3$ as

$$\begin{aligned}\frac{e^2}{3} \sum_{\mathbf{k}, \eta, \zeta} \frac{\eta}{k^2} \left[\left(\frac{m + \eta S}{\zeta E_k^\eta} \right)^3 - 1 \right] \int_0^\mu d\epsilon \delta(\epsilon - \eta S - \zeta E_k^\eta) &= \frac{e^2}{3} \sum_{\mathbf{k}, \eta} \Theta_\eta(\mu) \frac{\eta}{k^2} \left[\text{sign}(\mu) \left(\frac{m + \eta S}{E_k^\eta} \right)^3 - 1 \right] \\ &= \frac{e^2}{3} \frac{1}{2\pi^2} \sum_{\eta} \eta \Theta_\eta(\mu) \int_0^{\xi_\eta} dk \left[\text{sign}(\mu) \left(\frac{m + \eta S}{E_k^\eta} \right)^3 - 1 \right] \\ &= \frac{e^2}{3} \frac{1}{2\pi^2} \sum_{\eta} \eta \Theta_\eta(\mu) [\text{sign}(\mu)(m + \eta S) \tanh \theta_\eta^* - \xi_\eta] \\ &= -\frac{e^2}{3} \text{sign}(\mu) \sum_{\eta} \frac{\mu - m - 2\eta S}{(\mu - \eta S)^2} \eta \mathcal{N}_{0,0}^\eta(\mu),\end{aligned}\tag{D17}$$

where $\sinh \theta_\eta^* = \xi_\eta / (m + \eta S)$ because of $\Theta_\eta(\mu)$. Here we have used $\text{sign}(\mu) = \text{sign}(\mu - \eta S)$. Therefore, we obtain

$$\begin{aligned}\sigma_{xy}^{(3)} &= -\frac{Se^2}{3\pi^2} g(\lambda) - \frac{e^2}{6} \sum_\eta \eta \mathcal{N}_{0,0}^\eta(\mu) \frac{2 \text{sign}(\mu)(\mu - m - 2\eta S) + \mu + 2m + \eta S}{(\mu - \eta S)^2} \\ &= -\frac{Se^2}{3\pi^2} g(\lambda) - \frac{e^2}{12\pi^2} \sum_\eta \eta \Theta_\eta(\mu) \xi_\eta \frac{2 \text{sign}(\mu)(\mu - m - 2\eta S) + \mu + 2m + \eta S}{|\mu - \eta S|}.\end{aligned}\quad (\text{D18})$$

This is plotted in Fig. 5 (iii) as the Fermi-sea term for $\lambda = 0$.

Appendix E: Symmetry Relations

The relations in Eq. (61) are derived as follows. To be explicit, let us consider $Q_{ij}(i\omega_\lambda)$ given by Eq. (24). We insert $1 = UU^\dagger$ in all four interspaces in the trace, with $U = \rho_1$. Under this ‘unitary transformation’, the velocity matrix does not change, $U^\dagger \mathbf{v} U = \mathbf{v}$, while the Green’s function changes to

$$U^\dagger \tilde{G}_\mathbf{k}(i\epsilon_n; m, M, S, \mu) U = \tilde{G}_\mathbf{k}(i\epsilon_n; -m, -M, S, \mu) = -\tilde{G}_\mathbf{k}(-i\epsilon_n; m, M, -S, -\mu). \quad (\text{E1})$$

Note that the Green’s function $\tilde{G}_\mathbf{k}(i\epsilon_n)$ [Eq. (26)] explicitly includes the chemical potential μ . Note also that Eq. (E1) holds even in the presence of self-energy, Eq. (13), as can be seen from Feynman diagrams. By changing the variable as $i\epsilon_n \rightarrow i\omega_\lambda - i\epsilon_n$ and using the cyclic property of the trace, one can show that

$$Q_{ij}(i\omega_\lambda; \mu, M, S) = Q_{ji}(i\omega_\lambda; -\mu, M, -S). \quad (\text{E2})$$

This leads to

$$\sigma_{ij}(\mu, M, S) = \sigma_{ji}(-\mu, M, -S) \quad (\text{E3})$$

from Eq. (23). Since σ_{xy} is the anti-symmetric part of σ_{ij} , we obtain $\sigma_{xy}(\mu, M, S) = -\sigma_{xy}(-\mu, M, -S)$. This is the first equality in Eq. (61). The second equality in Eq. (61) follows if we note that σ_{xy} changes sign under $(M, S) \rightarrow (-M, -S)$. This can be shown in a similar way by taking $U = \sigma^y$ and changing variables as $(k_x, k_y, k_z) \rightarrow (-k_x, k_y, -k_z)$.

* E-mail address: jfujimoto@blade.mp.es.osaka-u.ac.jp

† E-mail address: kohno@s.phys.nagoya-u.ac.jp

¹ A.H. MacDonald and S.H. Vosko, J. Phys. C **12**, 2977 (1979).

² M.V. Ramana and A.K. Rajagopal, J. Phys. C **14**, 4291 (1981).

³ A. Crépieux and P. Bruno, Phys. Rev. B **64**, 014416 (2001); *ibid.* 094434.

⁴ For a review of *ab initio* approach, see H. Ebert, D. Ködderitzsch and J. Minár, Rep. Prog. Phys. **74**, 096501 (2011).

⁵ P.A. Wolff, J. Phys. Chem. Solids **25** 1057 (1964).

⁶ H. Zhang, C.-X. Liu, X.-L. Qi, X. Dai, Z. Fang, and S.-C. Zhang, Nature Phys. **5**, 438 (2009).

⁷ J. G. Checkelsky, J. Ye, Y. Onose, Y. Iwasa and Y. Tokura, Nature Physics **8**, 729 (2012).

⁸ Y. S. Hor *et al.*, Phys. Rev. B **81**, 195203 (2010).

⁹ C.-Z. Chang *et al.*, Science **340**, 167 (2013).

¹⁰ N. Samarth, private communication.

¹¹ W. Thomson, Proc. Royal Soc. London, **8**, 546 (1857).

¹² R.I. Potter, Phys. Rev. B **10**, 4626 (1974).

¹³ T.R. McGuire and R.I. Potter, IEEE Trans. Magn. **11** 1018 (1975).

¹⁴ S. Kokado, M. Tsunoda, K. Harigaya and A. Sakuma, J.

Phys. Soc. Jpn. **81** 024705 (2012).

¹⁵ E.H. Hall, Philos. Mag. **12**, 157 (1881).

¹⁶ R. Karplus and J. M. Luttinger, Phys. Rev. **95**, 1154 (1954).

¹⁷ N. Nagaosa, J. Sinova, S. Onoda, A. H. MacDonald, and N. P. Ong, Rev. Mod. Phys. **82**, 1539 (2011).

¹⁸ Particles with finite momentum \mathbf{k} more or less feel both \mathbf{M} and $-\mathbf{M}$.

¹⁹ Mathematically, under the Lorentz transformation, \mathbf{M} transforms as spatial components of an anti-symmetric tensor $\sigma^{\mu\nu} = [\gamma^\mu, \gamma^\nu]/2i$, where γ^μ ’s are Dirac gamma matrices, and can couple to an electromagnetic field $F_{\mu\nu}$. On the other hand, \mathbf{S} transforms as spatial components of a pseudo-vector $\gamma^5 \gamma^\mu$, but there is no physical pseudo-vector fields.

²⁰ Consider a system of interacting Dirac particles and applying to it a mean-field approximation. It is true that when the ferromagnetism arises from the Hartree-type mean field in the dipole-dipole interaction, which is mediated by real magnetic field, the order parameter should be \mathbf{M} . However, when the ferromagnetism arises, as in the nonrelativistic case, from the Fock-type mean field in the Coulomb interaction (or any other interactions), there is no reason to prefer \mathbf{M} over \mathbf{S} .

- ²¹ In the “effective” Dirac model, while the electromagnetic minimal coupling leads to a coupling, $-\mathbf{M}\cdot\mathbf{B}$, between \mathbf{M} and the magnetic field \mathbf{B} , there can be other couplings due to non-minimal couplig. For example, if $\boldsymbol{\sigma}$ corresponds to the real spin and is associated with a magnetic moment $g\mu_B\boldsymbol{\sigma}$ (instead of $g\mu_B\boldsymbol{\sigma}\rho_3$), there should be a direct Zeeman coupling, $-g\mu_B\boldsymbol{\sigma}\cdot\mathbf{B} \sim -\mathbf{S}\cdot\mathbf{B}$ between \mathbf{S} and \mathbf{B} .
- ²² A. K. Nguyen, H. J. Skadsem and A. Brataas, Phys. Rev. Lett. **98**, 146602 (2007).
- ²³ C. M. Wang, Phys. Rev. B **82**, 165331 (2010).
- ²⁴ R. Kubo, J. Phys. Soc. Jpn. **12**, 570 (1957).
- ²⁵ P. Středa, J. Phys. C **15**, L717 (1982).
- ²⁶ Generally, $\sigma_{xy}^{(2)}$ defined by Eq. (29) can contain intrinsic contributions due to “interband coherence”,^{32–34} and they are $\mathcal{O}(\gamma^0)$. In the present model, there are no contributions of $\mathcal{O}(\gamma^0)$ in the numerator while the denominator is $\mathcal{O}(\gamma)$, hence no intrinsic contribution in $\sigma_{xy}^{(2)}$.
- ²⁷ In the derivation, we noted that $D'' \equiv \text{Im}D_{\mathbf{k}}(\epsilon + i\eta) = \eta(\partial_{\epsilon}D_{\mathbf{k}})$ for $\eta \rightarrow +0$, and (ii) $\text{sign}(D'') = \text{sign}(\partial_{\epsilon}D_{\mathbf{k}})$. From (ii), we have $\text{sign}(D'')|\partial_{\epsilon}D_{\mathbf{k}}| = \partial_{\epsilon}D_{\mathbf{k}}$. From (i), we neglected the term containing $\partial_{\epsilon}\text{sign}(D'') \propto \delta(\partial_{\epsilon}D_{\mathbf{k}})$. This is because this term then contains $\delta(\partial_{\epsilon}D_{\mathbf{k}})\delta(D_{\mathbf{k}})$, which vanish if the equation $D(\epsilon) = 0$ does not have multiple root(s) as in the present case. (Note that there are no band crossings for the parameters we use in this paper.)
- ²⁸ L.L. Foldy and S.A. Wouthuysen, Phys. Rev. **78**, 29 (1950).
- ²⁹ S. Tani, Prog. Theor. Phys. **6**, 267 (1951).
- ³⁰ Equation (60) is loosely written by mixing real and \mathbf{k} -spaces, and as if V_{imp} conserves momentum, to avoid notational complications which are not essential here.
- ³¹ A similar concept of spin-dependent band width has been considered in, J. E. Hirsch, Phys. Rev. B **59**, 6256 (1999).
- ³² J. M. Luttinger and W. Kohn, Phys. Rev. **97**, 869 (1955).
- ³³ J. M. Luttinger, Phys. Rev. **112**, 739 (1958).
- ³⁴ N. Sinitsyn, A. H. MacDonald, T. Jungwirth, V. Dugaev, and J. Sinova, Phys. Rev. B **75**, 045315 (2007).